

## Enhancement of catalytic activity of lipase-immobilized Fe<sub>3</sub>O<sub>4</sub>-chitosan microsphere for enantioselective acetylation of racemic 1-phenylethylamine

Jiaying Pan<sup>\*</sup>, Zhimin Ou<sup>\*,†</sup>, Lan Tang<sup>\*</sup>, and Hanbing Shi<sup>\*\*\*,†</sup>

<sup>\*</sup>College of Pharmaceutical Science, Zhejiang University of Technology, Hangzhou, Zhejiang, China

<sup>\*\*</sup>The Third Affiliated Hospital of Qiqihar Medical College, Qiqihar, Heilongjiang, China

(Received 1 October 2018 • accepted 1 March 2019)

**Abstract**—Racemic 1-phenylethylamine was resolved by enantiomer selective acetylation using Fe<sub>3</sub>O<sub>4</sub>-chitosan microsphere (CTS)-glutaraldehyde-lipase in a solvent-free system under an alternating magnetic field. Magnetic chitosan microspheres (Fe<sub>3</sub>O<sub>4</sub>-CTS) were prepared via chemical co-precipitation and cross-linked with lipase using glutaraldehyde to form Fe<sub>3</sub>O<sub>4</sub>-CTS-glutaraldehyde-lipase particles. The magnetic, physicochemical, and textural characteristics of Fe<sub>3</sub>O<sub>4</sub>-CTS-glutaraldehyde-lipase particles were assessed by Fourier transform infrared spectroscopy, X-ray diffraction, and scanning electron microscopy. The optimal immobilization conditions were 2.4 mg/mL lipase, 10 mg/mL Fe<sub>3</sub>O<sub>4</sub>-CTS-glutaraldehyde, pH 8.5, 35 °C, 3 h. The loading amount of lipase and the specific activity got to 132 mg/g carrier and 48 U/g. The optimal reaction conditions of the acylation reaction using Fe<sub>3</sub>O<sub>4</sub>-CTS-glutaraldehyde-lipase were 300 mmol/L 1-phenylethylamine, 150 mg immobilized lipase, 2 mL vinyl acetate, 12.6 ×g rotating speed, 40 °C, 8 h. The activity of the Fe<sub>3</sub>O<sub>4</sub>-CTS-glutaraldehyde-lipase particles and conversion were improved when they were exposed to an external alternating magnetic field. The optimum magnetic field was 12 Gs (500 Hz). The conversion, enantiomeric excess of (*R*)-*N*-(1-phenylethyl)acetamide, and *E* value reached 41.8%, 98.4%, and 264, respectively. Fe<sub>3</sub>O<sub>4</sub>-CTS-glutaraldehyde-lipase could be reused seven times. A kinetic model of the immobilized lipase-catalyzed resolution of 1-phenylethylamine was set up based on the ping-pong bi-bi mechanism. The kinetic constants were  $V_{max}=1.62 \times 10^{-2}$  mM/min,  $K_A=2.84 \times 10^{-4}$  mM, and  $K_B=5.8 \times 10^{-1}$  mM. The model data fit well with the experimental data.

**Keywords:** Alternating Magnetic Field, Enantiomer Selective Acetylation, Fe<sub>3</sub>O<sub>4</sub>-CTS-glutaraldehyde-lipase, Solvent-free System, (*R*)-*N*-(1-phenylethyl)acetamide

### INTRODUCTION

Chiral amines and their derivatives, especially in the enantiopure form, are valuable building blocks for the synthesis of fine chemicals and final products in pharmaceutical and agrochemical industries [1,2]. They are also useful as resolving agents for enantiomer separation via diastereomeric salt formation, and as ligands for asymmetric synthesis via either transition metal catalysis or organocatalysis. The majority of pharmaceutical drugs are amines or their derivatives, and if chiral, their application in a non-racemic form is of paramount importance [3]. (*S*)-Phenylethylamine is a chiral raw material whose intermediates can be used in the preparation of optically active ketorolac, chiral 3,5-disubstituted-1',2',4'-triazole-[3',4'-b] diazines and diethylzinc, and also as chiral phosphorus reagents for asymmetric reactions of aromatic aldehydes [4-6].

Biocatalysis provides a fair balance in terms of efficiency, environmental friendliness, and cost [7]. There are several methods for obtaining enantiomerically pure compounds; lipases are ubiquitous enzymes and have been widely applied in industry because of their ability to catalyze enantioselective biotransformations [8]. Lipases (EC 3.1.1.3) are an important class of enzymes because of their regional specificity, stereospecificity and substrate specificity. In addition,

the mild catalysis conditions reduce the energy requirements [9]. Lipases catalyze many different reactions, although they are naturally designed to cleave ester bonds of triglycerides and subsequently release free fatty acids, diglycerides, monoglycerides, and glycerol [1-4]. Lipases can also catalyze the reverse reaction under mild aqueous conditions, i.e., formation of esters by reaction of alcohol and carboxylic acid moieties [10]. In recent years, these enzymes have been used in organic synthesis and for kinetic resolution of racemic compounds [11,12].

Although the lipase-catalyzed biotransformations in the presence or absence of organic solvents have been widely studied, enantioselective *N*-acylations under solvent-free conditions are rare and important [13,14]. Solvent-free systems offer many advantages such as minimal environmental impact and cost of solvent recovery and recycling, high enzyme stability, and fewer purification steps [15]. Furthermore, the utilization of solvent-free systems dramatically reduces the process hazards accompanying solvent exposure, toxicity, and flammability. Such developments can shift the manufacturing process towards a green, environmentally friendly route [16]. The absence of solvents also facilitates downstream processing and reduces the overall production cost [17].

It is difficult for free enzymes to be recovered and reused. As free enzymes have short operational lifetimes, massive amounts of the enzymes are wasted when utilized as such [18]. On the other hand, solid catalysts can be easily separated from the system after the reaction and may also be reused. The main obstacle to using

<sup>†</sup>To whom correspondence should be addressed.

E-mail: oozmm@163.com, shi-hanbing@163.com

Copyright by The Korean Institute of Chemical Engineers.

lipases in these applications is the cost of biocatalysts. One of the main goals of biocatalysis is to immobilize the maximum amount of the enzyme and retain its maximum activity at the lowest cost [19]. The immobilization of lipases on solid materials not only improves the life and stability of the biocatalysts, but also facilitates their recovery, reuse, and continuous enzymatic operation. It also protects the enzyme from solvent denaturation and improves its thermal stability [20].

Among the various immobilization methods, adsorption is the simplest and also the gentlest approach. It is the most direct method of immobilization, involving convenient experimental procedures. Furthermore, high enzyme loading and enhanced stability can be obtained via adsorption [21,22]. However, the weak forces between the enzyme molecules and the support material cause the adsorbent to continuously leach from the support, resulting in poor stability [23]. To overcome this problem, covalent connections should be used for immobilization. Lipases have been covalently linked to carriers having functional groups such as an aldehyde [24] or an

epoxy [25].  $\text{Fe}_3\text{O}_4$  nanoparticles exhibit unique properties including superparamagnetism and low toxicity [26,27]. They have been used as a support for immobilized enzymes because of associated advantages of easy separation and efficient cycling under external magnetic fields [28,29]. Chitosan, poly[*b*-(1-4)-link-2-amino-2-deoxy-D-glucose], is non-toxic, hydrophilic, biocompatible, biodegradable, and antibacterial, and available as a magnetic carrier; because it has different functional groups, it can be adjusted according to the specific application [30,31]. In addition, glutaraldehyde activation is a simple and effective method of immobilizing enzymes. Glutaraldehyde can react with several functional groups such as amino of proteins and supports [32,33]. Each glutaraldehyde is expected to form a Schiff base upon nucleophilic attack by the enzyme and the primary amino group in chitosan, and the stability of the enzyme is improved because of the bond formed by the Schiff base reaction [34,35]. In this work, magnetic chitosan microspheres (CTS) were synthesized by chemical co-precipitation [36,37].  $\text{Fe}_3\text{O}_4$ -CTS-glutaraldehyde-lipase particles were prepared by cross-link-

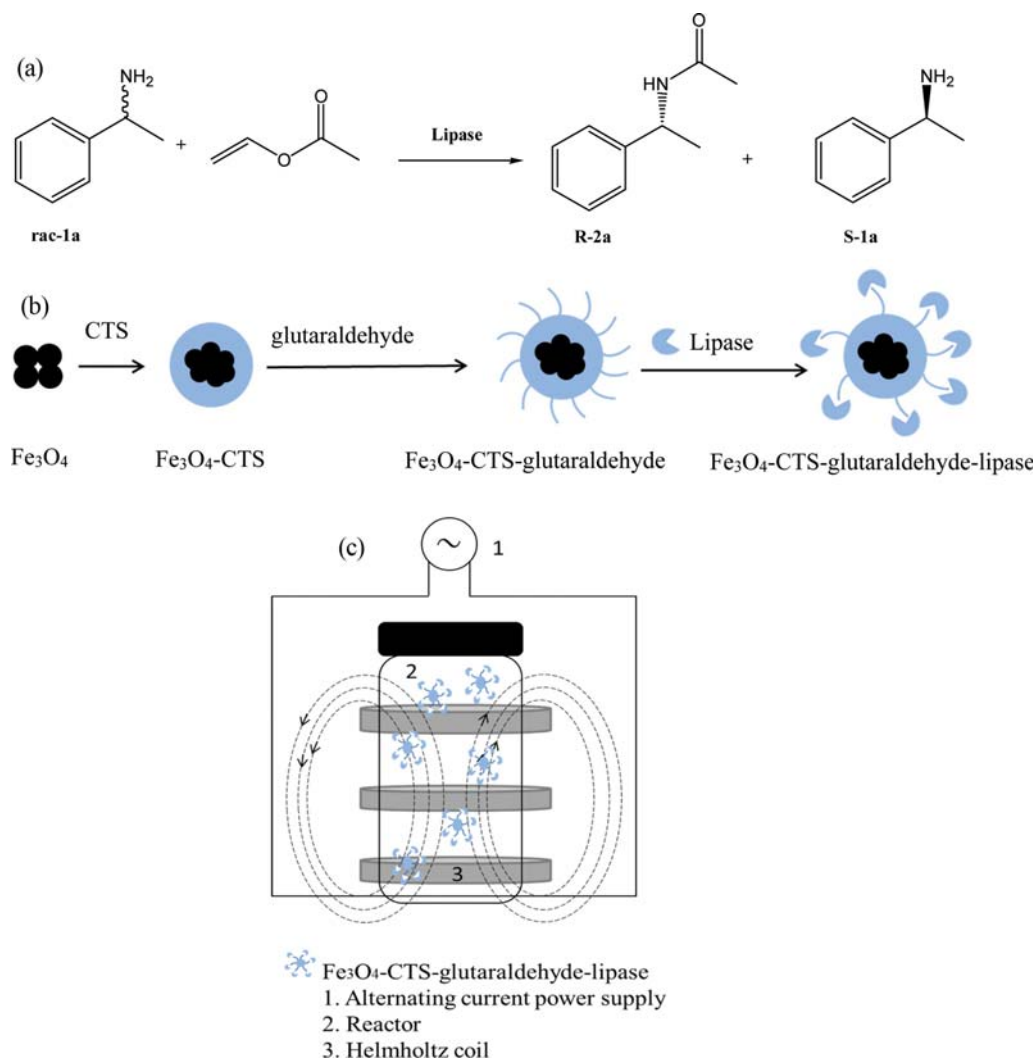


**Fig. 1.** Resolution of racemic 1-phenylethylamine (rac-1a) with lipase (a) (R-2a: (R)-N-(1-phenylethyl)acetamide; S-1a: (S)-phenylethylamine); Schematic illustration of the synthesis of  $\text{Fe}_3\text{O}_4$ -CTS-glutaraldehyde-lipase (b); Schematic diagram of the catalytic reaction by  $\text{Fe}_3\text{O}_4$ -CTS-glutaraldehyde-lipase in an alternating magnetic field (c).

ing Fe<sub>3</sub>O<sub>4</sub>-CTS and lipase using glutaraldehyde. The magnetic, physicochemical, and textural characteristics of Fe<sub>3</sub>O<sub>4</sub>-CTS-glutaraldehyde-lipase were studied by Fourier transform infrared spectroscopy (FT-IR), X-ray diffraction (XRD), and scanning electron microscopy (SEM).

There is a certain diffusion limitation in the immobilized enzyme catalyzed reaction, and the usual mechanical agitation is liable to damage the enzyme. A magnetic field can be applied to the catalytic reaction of the magnetic immobilized enzyme and used instead of mechanical stirring to improve the stirring mode [38,39]. The magnetic coil generates an external magnetic field that affects the magnetic immobilized enzyme, thereby increasing the reaction rate [40]. The direction of the alternating magnetic field is constantly changing and the magnetic carriers move in accordance with the direction of the magnetic field [41].

In this study, racemic 1-phenylethylamine (*rac-1a*) was resolved by enantiomer selective acetylation with Fe<sub>3</sub>O<sub>4</sub>-CTS-glutaraldehyde-lipase in a solvent-free system under an alternating magnetic field (Fig. 1(a)). The preparation conditions of Fe<sub>3</sub>O<sub>4</sub>-CTS-glutaraldehyde-lipase were optimized. Furthermore, the reaction conditions for optical resolution were also optimized with vinyl acetate as an acylating agent in a solvent-free system. A kinetic model was set up for the resolution of *rac-1a*.

## MATERIAL AND METHODS

### 1. Materials

Ferric chloride hexahydrate (FeCl<sub>3</sub>·6H<sub>2</sub>O), ferrous sulfate heptahydrate (FeSO<sub>4</sub>·7H<sub>2</sub>O), 95% deacetylated chitosan powder, racemic 1-phenylethylamine (*rac-1a*), vinyl acetate (99.5%), ammonia solution, and glutaraldehyde (50%) were purchased from Shanghai Aladdin Bio-Chem Technology Co., Ltd. Lipase (*Aspergillus niger*, specific activity 60 U/g) powder was purchased from HeNan Yangshao Bio-chem Engineering Co., Ltd., China. All other materials were of analytical grade.

### 2. Analytical Methods

The sample was analyzed by gas chromatography (GC) using a Shimadzu GC-2014 gas chromatograph equipped with a Hydrodex CP7502 column (Machery-Nagel; 25 m×0.25 mm×0.25 mm); FID temperature: 250 °C, injector temperature: 250 °C, H<sub>2</sub> pressure: 83 kPa, split ratio: 1 : 15. GC data (oven program: 100 °C, 13 min, 100-150 °C, 10 °C min<sup>-1</sup>, 10 min at 150 °C), tr (min): 7.9 [(S)-**1a**], 8.2 [(R)-**1a**], 22.7 [(R)-**2a**], 23.4 [(S)-**2a**].

The conversion (*c*), enantiomeric excess (*ee*), and enantiomeric ratio (*E*) were determined by gas chromatography. Conversion is defined as the ratio of the converted substrate concentration to the total substrate concentration.

The value of *E* was calculated from *c* and the enantiomeric excess of the product (*eeP*) using Eq. (1) [42].

$$E = \ln[1 - c(1 + eeP)] / \ln[1 - c(1 - eeP)] \quad (1)$$

The protein content of the lipase solution was determined by the Bradford method [43]. Loading amount of lipase (mg/g carrier) is defined as the protein content of immobilized enzyme on one unit mass carrier. The enzyme activity was determined by the acylation reaction of 600 mmol/L (or 300 mmol/L) *rac-1a* catalyzed by

20 mg of free lipase (or 150 mg of immobilized lipase) at 35 °C (or 40 °C) for 8 h in the shaken (12.6 ×g). The amount of the product (*R*)-*N*-(1-phenylethyl)acetamide formed was analyzed by GC analysis. One lipase unit (1 U) is defined as the amount of required enzyme to produce 1 mmol (*R*)-*N*-(1-phenylethyl)acetamide per hour under assay conditions. Specific activity is defined as enzyme activity divided by the number of milligrams of enzyme protein on the immobilized carrier.

### 3. Preparation of Fe<sub>3</sub>O<sub>4</sub>-CTS Particles

Fe<sub>3</sub>O<sub>4</sub>-CTS particles were prepared by chemical coprecipitation of Fe<sup>2+</sup> and Fe<sup>3+</sup> ions by treating with NH<sub>3</sub>·H<sub>2</sub>O in the presence of chitosan. In a typical procedure, 2 g of chitosan was dissolved in 100 mL of 2% acetate acid solution, and Fe<sup>2+</sup> and Fe<sup>3+</sup> (molar ratio of 1 : 2) were dissolved in the solution. This solution was chemically precipitated at 40 °C by adding NH<sub>3</sub>·H<sub>2</sub>O dropwise with vigorous stirring under the protection of nitrogen. The suspension was heated to 80 °C and the temperature was maintained for 1 h under continuous stirring. The Fe<sub>3</sub>O<sub>4</sub>-chitosan particles were then separated with an external magnet, rinsed several times with water, and dried at 60 °C under vacuum [27].

### 4. Immobilization of Lipase onto Fe<sub>3</sub>O<sub>4</sub>-CTS Particles

Before the immobilization of lipase onto Fe<sub>3</sub>O<sub>4</sub>-CTS particles, the primary amino groups of the microspheres were activated using glutaraldehyde coupling agent. Lipase was covalently immobilized on Fe<sub>3</sub>O<sub>4</sub>-CTS by forming a Schiff base linkage between the aldehyde group of glutaraldehyde and the terminal amino group of lipase [33]. In a typical procedure, 500 mg of dry magnetic chitosan microspheres was mixed with 0.75 mL glutaraldehyde solution in 47.25 mL phosphate buffer at pH 7.0, and the reaction was allowed to proceed at 30 °C for 4 h. The glutaraldehyde-activated particles were subsequently recovered by magnetic separation and then washed with distilled water. The activated magnetic carriers had reactive aldehyde groups that could react with the amino groups of lipase to form covalent bonds.

The Fe<sub>3</sub>O<sub>4</sub>-CTS-glutaraldehyde activated particles were transferred to 50 mL of 2.4 mg/mL lipase solution in 0.1 M phosphate buffer at pH 8.5. The above mixture was agitated at 35 °C for 3 h. After the completion of the immobilization reaction, the immobilized lipase was separated by application of an external magnetic field. The obtained precipitates were washed carefully with phosphate buffer several times until unbound lipase was completely removed. The immobilized lipase was frozen in an ultra-low temperature freezer (−80 °C) for 8 h. The sample bottle containing frozen lipase was sealed by a sealing film with holes by puncture and dried by lyophilization for 12 h (Fig. 1(b)) [38].

### 5. Characterization of Fe<sub>3</sub>O<sub>4</sub>, Fe<sub>3</sub>O<sub>4</sub>-CTS, and Fe<sub>3</sub>O<sub>4</sub>-CTS-glutaraldehyde-lipase

The FT-IR spectra of the lipase-immobilized magnetic particles and free lipase were obtained using an FT-IR spectrophotometer (iS50, Nicolet). The surface features of Fe<sub>3</sub>O<sub>4</sub>, Fe<sub>3</sub>O<sub>4</sub>-CTS, and Fe<sub>3</sub>O<sub>4</sub>-CTS-glutaraldehyde-lipase were evaluated by a field emission scanning electron microscope (SEM) (S-4700, Hitachi). Fe<sub>3</sub>O<sub>4</sub>, Fe<sub>3</sub>O<sub>4</sub>-CTS, Fe<sub>3</sub>O<sub>4</sub>-CTS-glutaraldehyde, and Fe<sub>3</sub>O<sub>4</sub>-CTS-glutaraldehyde-lipase were analyzed by X-ray powder diffraction (XRD). XRD measurements were conducted on a Rigaku D/MAX-3B X-ray diffractometer employing Cu K $\alpha$  radiation ( $\lambda$ =0.1542 nm).

## 6. Optimization of the Preparation Conditions for Fe<sub>3</sub>O<sub>4</sub>-CTS-glutaraldehyde-lipase

As a higher conversion in the acetylation of racemic 1-phenylethylamine implies a higher activity of Fe<sub>3</sub>O<sub>4</sub>-CTS-glutaraldehyde-lipase, we decided to use it to indicate the activity of Fe<sub>3</sub>O<sub>4</sub>-CTS-glutaraldehyde-lipase in this study.

In a glass vial with a screw cap, 150 mg of the Fe<sub>3</sub>O<sub>4</sub>-CTS-glutaraldehyde-lipase sample was added to a 2 mL vinyl acetate solution containing 300 mmol/L of *rac*-1a. The mixture was shaken (12.6 ×g) at 40 °C for 8 h. Samples were collected directly from the reaction mixture after 8 h and analyzed by GC.

### 6-1. Optimization of Initial Free Lipase Concentration used for Immobilization

To optimize the initial free lipase concentration for immobilization, 0.8, 1.6, 2.4, 3.2, 4.0, and 4.8 mg/mL lipase solutions were added to the reactors containing 500 mg of Fe<sub>3</sub>O<sub>4</sub>-CTS-glutaraldehyde. After shaking the reactor at 35 °C and 12.6 ×g for 3 h, Fe<sub>3</sub>O<sub>4</sub>-CTS-glutaraldehyde-lipases were precipitated using a magnet and washed with 0.1 mol/L phosphate buffer solution (pH=7.0). The Fe<sub>3</sub>O<sub>4</sub>-CTS-glutaraldehyde-lipases were then repeatedly washed with absolute ethanol and ultrapure water several times before finally drying by lyophilization.

### 6-2. Determination of Optimal pH Value of the Buffer for Immobilization

In the pH optimization experiments, 2.4 mg/mL lipase solutions were put into seven reactors containing 500 mg of Fe<sub>3</sub>O<sub>4</sub>-CTS-glutaraldehyde and 50 mL of pH 6.0, 6.5, 7.0, 7.5, 8.0, 8.5, and 9.0 phosphate buffer solutions. After shaking at 35 °C and 12.6 ×g for 3 h, Fe<sub>3</sub>O<sub>4</sub>-CTS-glutaraldehyde-lipase powders were precipitated using a magnet and washed with 0.1 mol/L phosphate buffer solution (pH=6.0, 6.5, 7.0, 7.5, 8.0, 8.5, and 9.0). The powders were then washed with absolute ethanol and ultrapure water several times, and finally dried by lyophilization.

### 6-3. Determination of the Optimum Time for Immobilization

To optimize the immobilization reaction time, 2.4 mg/mL of lipase was put into five reactors containing 500 mg of Fe<sub>3</sub>O<sub>4</sub>-CTS-glutaraldehyde and 50 mL pH 8.5 phosphate buffer solution. After shaking the reactor at 35 °C and 12.6 ×g for 1, 2, 3, 4, and 5 h, Fe<sub>3</sub>O<sub>4</sub>-CTS-glutaraldehyde-lipases were precipitated with a magnet and washed with 0.1 mol/L phosphate buffer solution (pH=8.5), and then repeatedly washed with absolute ethanol and ultrapure water several times. Finally, the Fe<sub>3</sub>O<sub>4</sub>-CTS-glutaraldehyde-lipases were dried by lyophilization.

### 6-4. Determination of the Optimal Temperature for Immobilization

For optimization of the immobilization reaction temperature, 2.4 mg/mL lipase solutions were put into five reactors containing 500 mg of Fe<sub>3</sub>O<sub>4</sub>-CTS-glutaraldehyde and 50 mL pH 8.5 phosphate buffer solution. After shaking at 25, 30, 35, 40, and 45 °C at 12.6 ×g for 3 h, the Fe<sub>3</sub>O<sub>4</sub>-CTS-glutaraldehyde-lipase powders were precipitated using a magnet and washed with 0.1 mol/L phosphate buffer (pH=8.5) solution, and then repeatedly washed with absolute ethanol and ultrapure water several times. Finally, the immobilized lipase powders were dried by lyophilization.

## 7. Optimization of the Acetylation Reaction Conditions

### 7-1. Optimization of Reaction Temperature for Acetylation

150 mg of Fe<sub>3</sub>O<sub>4</sub>-CTS-glutaraldehyde-lipase contains 20 mg of

free lipase. In a glass vial with a screw cap, 150 mg of Fe<sub>3</sub>O<sub>4</sub>-CTS-glutaraldehyde-lipase or 20 mg free lipase was added to a 2 mL vinyl acetate solution containing 300 mmol/L *rac*-1a. The mixture was shaken (12.6 ×g) at 25, 30, 35, 40, 45, or 50 °C for 8 h. Samples were analyzed by GC.

### 7-2. Optimization of the amount of the Enzyme for Acetylation

In a glass vial with a screw cap, 100, 150, 200, 250, and 300 mg of Fe<sub>3</sub>O<sub>4</sub>-CTS-glutaraldehyde-lipase were added to a 2 mL vinyl acetate solution containing 300 mmol/L *rac*-1a. The mixture was shaken at 12.6 ×g and 40 °C. Samples were analyzed by GC after 8 h.

In a glass vial with a screw cap, 10, 15, 20, 25, or 30 mg of free lipase was added to a 2 mL vinyl acetate solution containing 300 mmol/L *rac*-1a. The mixture was shaken at 12.6 ×g and 35 °C. Samples were analyzed by GC after 8 h.

### 7-3. Optimization of Substrate Concentration for Acetylation

In a glass vial with a screw cap, 150 mg of Fe<sub>3</sub>O<sub>4</sub>-CTS-glutaraldehyde-lipase was added to a 2 mL vinyl acetate solution containing 100, 200, 300, 400, 500, 600, 800, and 1,000 mmol/L *rac*-1a. The mixture was shaken at 12.6 ×g and 40 °C. Samples were analyzed by GC after 8 h.

In a glass vial with a screw cap, 20 mg of free lipase was added to a 2 mL vinyl acetate solution containing 100, 200, 300, 400, 500, 600, 800, and 1,000 mmol/L *rac*-1a. The mixture was shaken at 12.6 ×g and 35 °C. Samples were analyzed by GC after 8 h.

### 7-4. Optimization of Shaker Incubator Speed for Acetylation

In a glass vial with a screw cap, 150 mg of Fe<sub>3</sub>O<sub>4</sub>-CTS-glutaraldehyde-lipase was added to a 2 mL vinyl acetate solution containing 300 mmol/L *rac*-1a. The mixture was shaken at 40 °C and 1.4 ×g, 5.6 ×g, 12.6 ×g, 22.4 ×g, and 35 ×g. Samples were analyzed by GC after 8 h.

In a glass vial with a screw cap, 20 mg of free lipase was added to a 2 mL vinyl acetate solution containing 600 mmol/L *rac*-1a. The mixture was shaken at 35 °C and 1.4 ×g, 5.6 ×g, 12.6 ×g, 22.4 ×g, and 35 ×g. Samples were analyzed by GC after 8 h.

## 8. Effect of Magnetic Field Strength on the Activity of Fe<sub>3</sub>O<sub>4</sub>-CTS-glutaraldehyde-lipase

An alternating magnetic field was generated by a lab-made device. A schematic diagram of the device constructed for generating an electromagnetic alternating field is illustrated in Fig. 1(c). The strength and frequency of the magnetic field could be adjusted. The reactions were conducted under an alternating magnetic field with a specific frequency of 500 Hz. The acylation reaction using Fe<sub>3</sub>O<sub>4</sub>-CTS-glutaraldehyde-lipase as the catalyst was carried out under an external magnetic field for 8 h. The applied magnetic field strengths were 4, 8, 12, 16, and 20 Gs. The conversion of the acylation reaction was investigated with respect to the changing magnetic field strength.

## 9. Reuse of Fe<sub>3</sub>O<sub>4</sub>-CTS-glutaraldehyde-lipase or Free Lipase in Acetylation Reaction

In a glass vial with a screw cap, 150 mg of Fe<sub>3</sub>O<sub>4</sub>-CTS-glutaraldehyde-lipase was added to 2 mL of the vinyl acetate solution containing 300 mmol/L *rac*-1a. The reaction was carried out at 40 °C for 8 h under an alternating electromagnetic field (12 Gs).

In a glass vial with a screw cap, 20 mg of free lipase was added to a 2 mL vinyl acetate solution containing 300 mmol/L of *rac*-1a. The mixture was shaken at 35 °C and 12.6 ×g for 8 h.

Fe<sub>3</sub>O<sub>4</sub>-CTS-glutaraldehyde-lipase or free lipase powders were

collected by centrifugation after the end of the above reaction, the obtained precipitates were washed carefully with vinyl acetate for five times until substrate and product was completely removed and reused for the acetylation reaction seven times. Samples were analyzed by GC.

### 10. Kinetic Model for Enantiomer-selective Acylation of *rac*-1a

Time-course measurements of the catalytic reaction were performed in a 10 mL glass vial with 2 mL vinyl acetate containing 100, 150, 200, 250 and 300 mmol/L *rac*-1a and 150 mg of Fe<sub>3</sub>O<sub>4</sub>-CTS-glutaraldehyde-lipase as catalyst under an alternating electromagnetic field. 20  $\mu$ L aliquots of the well-stirred reaction mixture were withdrawn in intervals for GC analysis.

## RESULTS AND DISCUSSION

### 1. Characterization of Fe<sub>3</sub>O<sub>4</sub> Nanoparticles, Fe<sub>3</sub>O<sub>4</sub>-CTS, and Fe<sub>3</sub>O<sub>4</sub>-CTS-glutaraldehyde-lipase

The FT-IR spectra of Fe<sub>3</sub>O<sub>4</sub> nanoparticles, Fe<sub>3</sub>O<sub>4</sub>-CTS, Fe<sub>3</sub>O<sub>4</sub>-CTS-glutaraldehyde-lipase, and free lipase are presented in Fig. 2(a). The characteristic absorption peak for Fe<sub>3</sub>O<sub>4</sub> was observed at 576

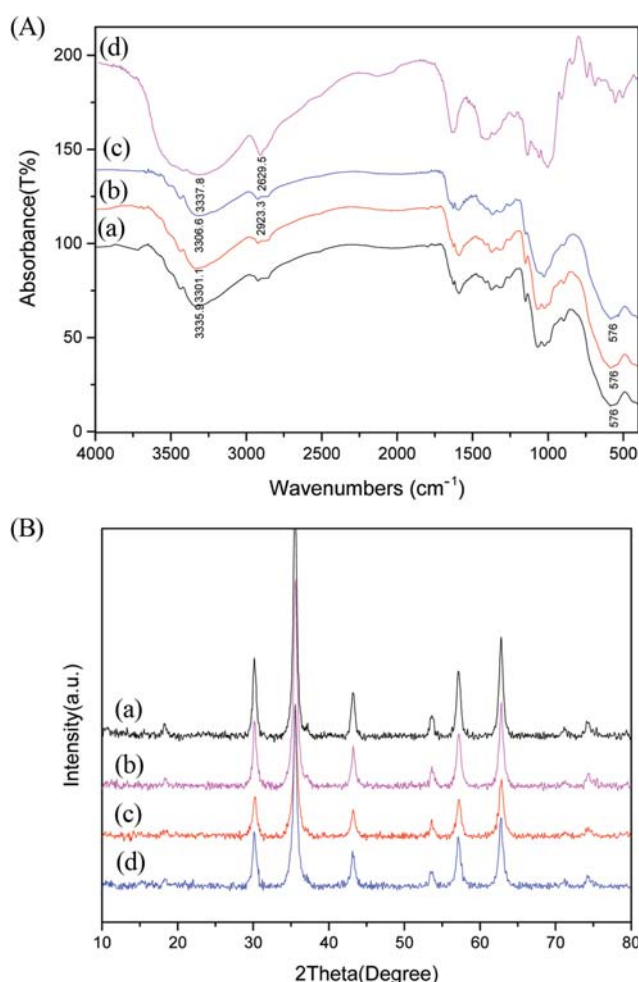


Fig. 2. (A) FT-IR spectra of Fe<sub>3</sub>O<sub>4</sub> (a); Fe<sub>3</sub>O<sub>4</sub>-CTS-glutaraldehyde (b); Fe<sub>3</sub>O<sub>4</sub>-CTS-glutaraldehyde-lipase (c) and the free lipase (d); (B) XRD patterns for Fe<sub>3</sub>O<sub>4</sub> (a), Fe<sub>3</sub>O<sub>4</sub>-CTS (b), Fe<sub>3</sub>O<sub>4</sub>-CTS-glutaraldehyde (c); Fe<sub>3</sub>O<sub>4</sub>-CTS-glutaraldehyde-lipase (d).

cm<sup>-1</sup> (Fe-O), which indicated that the preparation of Fe<sub>3</sub>O<sub>4</sub> nanoparticles was successful and Fe<sub>3</sub>O<sub>4</sub> existed in the structure of Fe<sub>3</sub>O<sub>4</sub>-CTS and Fe<sub>3</sub>O<sub>4</sub>-CTS-glutaraldehyde-lipase. The characteristic adsorption bands appeared at 3,300, 2,920 and 1,066 cm<sup>-1</sup> corresponding to the bending vibration of N-H and partially O-H group, aliphatic C-H and bending vibrations of C-O in the chitosan respectively. Similar results were also reported by Wang et al. [27] and Baghban et al. [44].

The structures of Fe<sub>3</sub>O<sub>4</sub> nanoparticles, Fe<sub>3</sub>O<sub>4</sub>-CTS, Fe<sub>3</sub>O<sub>4</sub>-CTS-glutaraldehyde and Fe<sub>3</sub>O<sub>4</sub>-CTS-glutaraldehyde-lipase were characterized by XRD. As shown in Fig. 2(b), the six characteristic peaks of Fe<sub>3</sub>O<sub>4</sub> (a) were observed at  $2\theta=30.17^\circ$ ,  $35.66^\circ$ ,  $43.38^\circ$ ,  $53.85^\circ$ ,  $57.31^\circ$ , and  $62.88^\circ$ , which corresponded to the (220), (311), (400), (422), (511), and (440) indices, respectively. These peaks revealed that the particles were pure Fe<sub>3</sub>O<sub>4</sub> with a spinel structure (JCPDS database, 79-0418). For the same six, characteristic peaks were also observed for Fe<sub>3</sub>O<sub>4</sub>-CTS, Fe<sub>3</sub>O<sub>4</sub>-CTS-glutaraldehyde and Fe<sub>3</sub>O<sub>4</sub>-CTS-glutaraldehyde-lipase [30]. Thus, it was evident that the immobilization process did not have a destructive effect on the crystal structure of magnetite. A small decrease in the intensity of these peaks showed that a non-magnetite structure (lipase) was added to the system. The magnetic particles could preserve their magnetic properties during the separation process, which is suitable for conducting bioseparation.

The enzyme-magnetic particle assemblies were characterized by SEM. It is evident from Fig. 3(a) that the Fe<sub>3</sub>O<sub>4</sub> nanoparticles were granular and that the dispersion of the Fe<sub>3</sub>O<sub>4</sub> nanoparticles was not ideal because of the interfacial effect of the nanoparticles and the formation of a large number of hydrogen bonds between the surface-rich hydroxyl groups. Fig. 3(b) is an enlarged SEM image of a Fe<sub>3</sub>O<sub>4</sub>-CTS microsphere. It can be clearly seen that the surface of the microsphere is rugged and has many folds. This morphology implies that the surface area of the microsphere is large and beneficial for the immobilization of the enzyme. Fig. 3(c) and 3(d) are the images of Fe<sub>3</sub>O<sub>4</sub>-CTS-glutaraldehyde-lipase. It was found that these particles were large with a rugged surface and a large specific surface area to facilitate the enzymatic reaction. The rigid structure of the magnetic carrier implies that it would have good pH, thermal, and storage stability [29].

### 2. Optimization of the Preparation Process for Fe<sub>3</sub>O<sub>4</sub>-CTS-glutaraldehyde-lipase

#### 2-1. Influence of the Initial Free Lipase Concentration on the Activity of Fe<sub>3</sub>O<sub>4</sub>-CTS-glutaraldehyde-lipase

The loading amount of lipase increased with the increase of the initial free lipase concentration. Specific activity first increased and then decreased. The chitosan microspheres have a certain number of active groups on the surface that can bind to lipase. The specific activity of the Fe<sub>3</sub>O<sub>4</sub>-CTS-glutaraldehyde-lipase would increase with the amount of the adsorbed enzyme if the combination of the active group of lipase is not saturated. Table 1 shows that the maximum of specific activity reached 42 U/g. The decreasing specific activity might be related to some active hidden sites caused by the aggregation of enzyme at high concentration when the loading amount of lipase was above 2.4 mg/mL [45]. Therefore, the optimal initial free lipase concentration was 2.4 mg/mL for 10 mg/mL Fe<sub>3</sub>O<sub>4</sub>-CTS-glutaraldehyde.

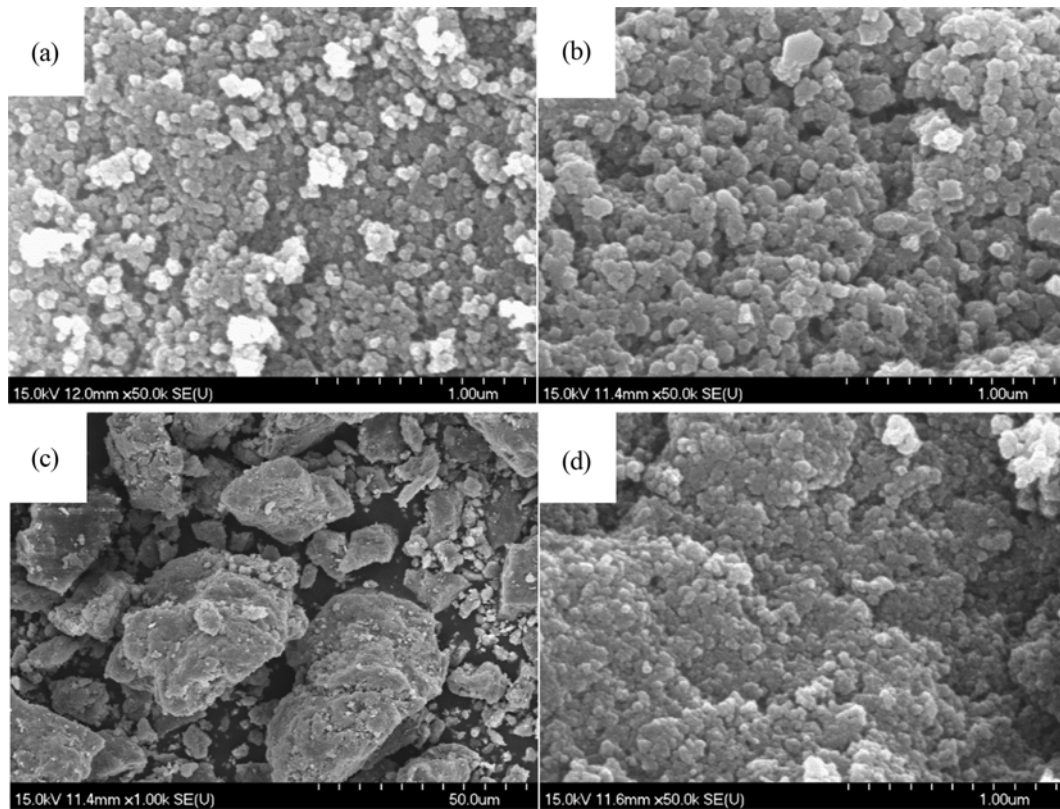


Fig. 3. SEM image of the surface of Fe<sub>3</sub>O<sub>4</sub> (a), Fe<sub>3</sub>O<sub>4</sub>-CTS (b), Fe<sub>3</sub>O<sub>4</sub>-CTS-glutaraldehyde-lipase (c), (d).

Table 1. Effect of initial free lipase concentration on the activity of Fe<sub>3</sub>O<sub>4</sub>-CTS-glutaraldehyde-lipase

Initial free lipase concentration (mg/mL)	Loading amount of lipase (mg/g carrier)	Specific activity (U/g)
0.8	59.2	32
1.6	98.8	38
2.4	115.2	42
3.2	116.1	38
4.0	116.5	35

Immobilization conditions: 10 mg/mL Fe<sub>3</sub>O<sub>4</sub>-CTS-glutaraldehyde, pH 7.0, 35 °C, 12.6 ×g, 3 h

Table 2. Effect of pH of buffer on the activity of Fe<sub>3</sub>O<sub>4</sub>-CTS-glutaraldehyde-lipase

pH	Loading amount of lipase (mg/g carrier)	Specific activity (U/g)
6.0	76.8	30
6.5	98.4	37
7.0	115.2	42
7.5	120.0	43
8.0	124.8	46
8.5	132.0	48
9.0	110.4	34

Immobilization conditions: 10 mg/mL Fe<sub>3</sub>O<sub>4</sub>-CTS-glutaraldehyde, 2.4 mg/mL initial free lipase concentration, 35 °C, 12.6 ×g, 3 h

Table 3. Effect of immobilization time on the activity of Fe<sub>3</sub>O<sub>4</sub>-CTS-glutaraldehyde-lipase

Time (h)	Loading amount of lipase (mg/g carrier)	Specific activity (U/g)
1	72.0	38
2	100.8	44
3	132.0	48
4	132.0	48
5	132.1	48

Immobilization conditions: 10 mg/mL Fe<sub>3</sub>O<sub>4</sub>-CTS-glutaraldehyde, 2.4 mg/mL initial free lipase concentration, pH 8.5, 35 °C, 12.6 ×g

Table 4. Effect of immobilization temperature on the activity of Fe<sub>3</sub>O<sub>4</sub>-CTS-glutaraldehyde-lipase

Temperature (°C)	Loading amount of lipase (mg/g carrier)	Specific activity (U/g)
25	76.8	38
30	105.6	40
35	132.0	48
40	132.0	30
45	132.4	18

Immobilization conditions: 10 mg/mL Fe<sub>3</sub>O<sub>4</sub>-CTS-glutaraldehyde, 2.4 mg/mL initial free lipase concentration, pH 8.5, 12.6 ×g for 3 h

## 2-2. Determination of the Optimal pH Value of the Buffer for Immobilization

Table 2 shows that the optimal pH value for immobilization is 8.5. The specific activity of Fe<sub>3</sub>O<sub>4</sub>-CTS-glutaraldehyde-lipase was affected by the pH value of the buffer. The ionization state of the enzyme molecule and that of the carrier were varied in different pH buffer so that the binding of the enzyme molecule to the carrier would be affected [27]. The changes of lipase structure will cause the enzyme to be inactivated after denaturation and the enzyme

activity will be lower when the pH exceeds a certain value.

## 2-3. Influence of the Immobilization Reaction Time on the Activity of Fe<sub>3</sub>O<sub>4</sub>-CTS-glutaraldehyde-lipase

With the prolongation of immobilization time, the loading amount of lipase increased, and the specific activity of Fe<sub>3</sub>O<sub>4</sub>-CTS-glutaraldehyde-lipase increased, as shown in Table 3. When the immobilization time was too short, lipase and the carrier did not bind strongly enough, which lowered the loading amount of lipase and specific activity of Fe<sub>3</sub>O<sub>4</sub>-CTS-glutaraldehyde-lipase. The loading

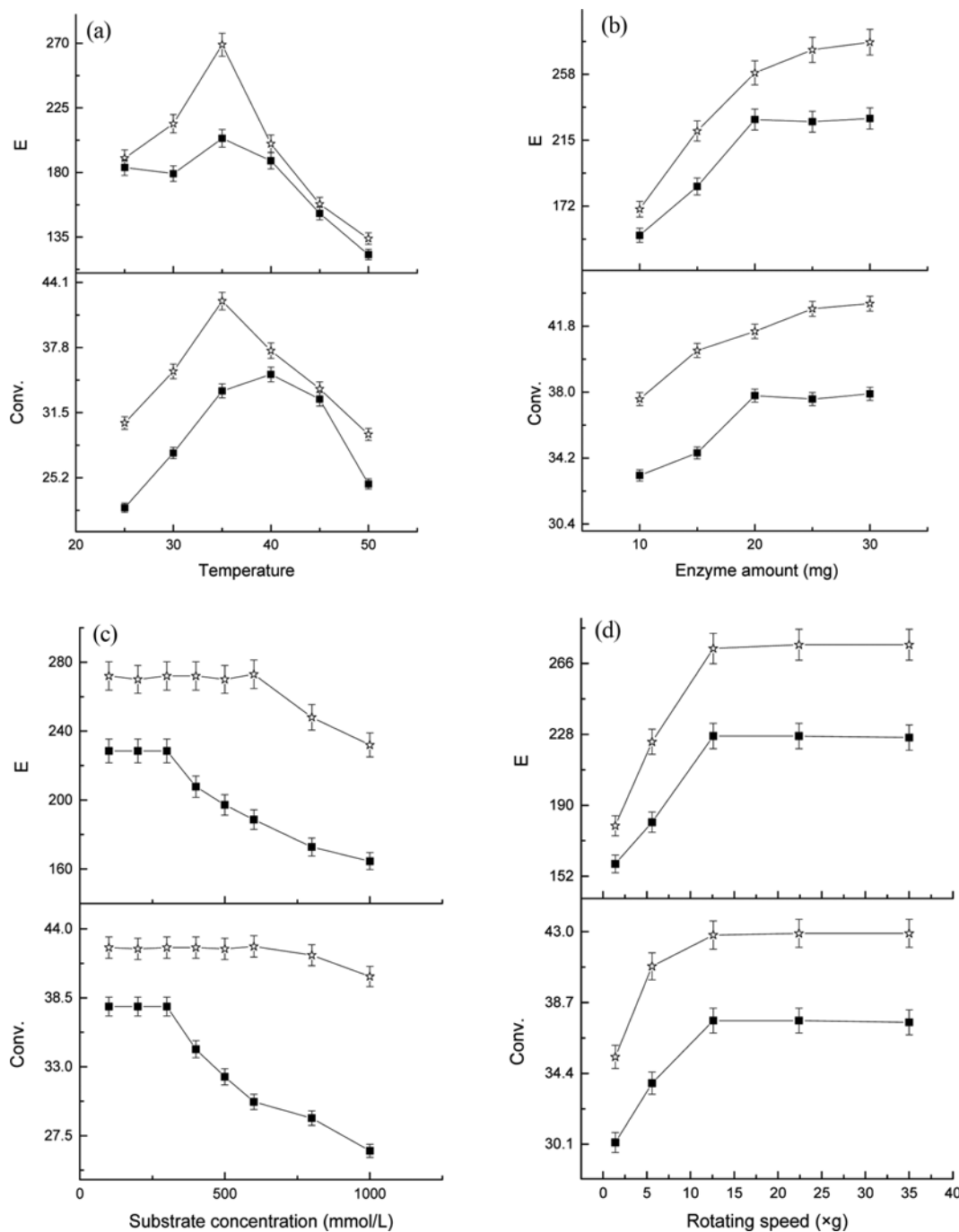


Fig. 4. Optimization of the enantiomer-selective acylation reaction conditions. Temperature (a); Enzyme amount (b); Substrate concentration (c); Rotating speed (d); Fe<sub>3</sub>O<sub>4</sub>-CTS-glutaraldehyde-lipase (■); Free lipase (☆).

amount of lipase reached 132 mg/g carrier within 3 h, and then remained nearly constant with prolonged incubation. This result is in accordance with that reported by Pan et al. [45]. The optimal immobilization time was 3 h.

#### 2-4. Influence of the Immobilization Temperature on the Activity of Fe<sub>3</sub>O<sub>4</sub>-CTS-glutaraldehyde-lipase

The loading amount of lipase and specific activity of Fe<sub>3</sub>O<sub>4</sub>-CTS-glutaraldehyde-lipase obtained by immobilization at lower temperatures was lower because the immobilization reaction not complete at low temperatures and the unit carrier was not saturated. With the increase in immobilization temperature, the reaction proceeded faster. However, when the immobilization reaction temperature reached 35 °C, the specific activity of the Fe<sub>3</sub>O<sub>4</sub>-CTS-glutaraldehyde-lipase clearly decreased (Table 4). This was attributed to the denaturation of the free enzyme in the system and its inactivation [46]. Furthermore, as described above, some of the inactivated enzyme molecules were immobilized on the carrier during the immobilization process, resulting in lower specific activity of Fe<sub>3</sub>O<sub>4</sub>-CTS-glutaraldehyde-lipase.

To summarize, the optimal immobilization conditions were 2.4 mg/mL lipase, 10 mg/mL of Fe<sub>3</sub>O<sub>4</sub>-CTS-glutaraldehyde, pH 8.5, 35 °C, 3 h. Under the optimal immobilization conditions, loading amount of lipase and the specific activity got to 132 mg/g carrier and 48 U/g.

### 3. Optimization of the Enantiomer-selective Acylation Reaction Conditions

#### 3-1. Influence of Reaction Temperature on Enantiomer Selective Acetylation

Fig. 4(a) shows that the optimal acetylation reaction temperatures for free lipase and Fe<sub>3</sub>O<sub>4</sub>-CTS-glutaraldehyde-lipase were 35 and 40 °C, respectively. The thermal stability of lipase increased after its immobilization. Because the free lipase and the surface-active groups of the microspheres formed a stable structure, which could protect the active center of the lipase, the critical temperature of the Fe<sub>3</sub>O<sub>4</sub>-CTS-glutaraldehyde-lipase was increased. The optimum reaction temperature of Fe<sub>3</sub>O<sub>4</sub>-CTS-glutaraldehyde-lipase was improved and the lipase enzyme could perform the enzymatic reaction at a higher temperature, thereby improving its application range.

#### 3-2. Influence of Enzyme amount on the Enantiomer Selective Acetylation

In the reactor, 300 mmol/L *rac*-**1a** was converted by 100 mg, 150 mg, 200 mg, 250 mg, and 300 mg of Fe<sub>3</sub>O<sub>4</sub>-CTS-glutaraldehyde-lipase, at 12.6 ×g and 40 °C. It is evident in Fig. 4(b) that the conversion was slower when 100 mg of Fe<sub>3</sub>O<sub>4</sub>-CTS-glutaraldehyde-lipase was used, but gradually increased with the increasing amount of Fe<sub>3</sub>O<sub>4</sub>-CTS-glutaraldehyde-lipase, indicating that the problem of internal diffusion was not the rate-limiting step in this system. As the addition of more lipase is beneficial to the conversion, the actual amount of the enzyme required for the reaction ought to be determined based on the cost relationship. When the substrate concentration was 300 mmol/L, most of (*R*)-**1a** could be converted to (*R*)-**2a** using 150 mg of Fe<sub>3</sub>O<sub>4</sub>-CTS-glutaraldehyde-lipase after 8 h.

#### 3-3. Influence of Substrate Concentration on Enantiomer-selective Acetylation

Different amounts (100, 200, 300, 400, 500, 600, 800, and 1,000 mmol/L) of *rac*-**1a** were added to the reactors to investigate the effect of substrate concentration on the enantiomer-selective acyla-

tion with Fe<sub>3</sub>O<sub>4</sub>-CTS-glutaraldehyde-lipase or free lipase as catalyst. Significant alterations were observed in the biocatalytic properties of lipase (Fig. 4(c)) in the resolutions of *rac*-**1a** between 100 mmol/L and 1,000 mmol/L. *ee*(*R*)-**2a** was high after 8 h when the substrate concentration was 100-300 mmol/L. The conversion of *rac*-**1a** reached a maximum of 37.8% when the substrate concentration was 300 mmol/L. However, the conversion of *rac*-**1a** showed a significant downward trend with further increase in substrate concentration. The substrate or intermediate tightly binds to the active site, and this step is the rate-determining; the reduced number of active sites could reduce the reaction rate or conversion yield. The presence of the carrier makes it difficult for the substrate to contact the active site of the immobilized lipase, resulting in a decrease of conversion at high substrate concentrations. At low substrate concentrations, the active site of lipase is not fully saturated and its catalytic potential is not fully exploited. With further increase in the substrate concentration, conversion decreases slightly, possibly owing to the substrate inhibition of enzyme activity. The optimal substrate concentrations were 600 mmol/L and 300 mmol/L using free lipase and Fe<sub>3</sub>O<sub>4</sub>-CTS-glutaraldehyde-lipase, respectively. The active site of the immobilized enzyme was completely saturated when the substrate concentration reached 300 mmol/L. Conversion decreased with the increase of substrate concentration.

#### 3-4. Optimum Rotating Speed of Shaker Incubator

The effect of rotating speed on the enantiomer-selective acylation of *rac*-**1a** was studied in reactors with 150 mg Fe<sub>3</sub>O<sub>4</sub>-CTS-glutaraldehyde-lipase and 300 mmol/L *rac*-**1a** at 40 °C and 1.4-35 ×g. Fig. 4(d) shows that the conversion, *ee*(*R*)-**2a** and *E* increased with the increasing rotating speeds ranging from 1.4-12.6 ×g. The conversion, *ee*(*R*)-**2a**, and *E* were stable when the rotating speed was above 12.6 ×g. At low speeds, most lipases were deposited at the bottom of the bottle and could not disperse throughout the reaction system and interact adequately with the substrates. The lipase distribution in the reactor improved as the rotating speed increased. A high-enough rotating speed could eliminate the effect of external diffusion on the enzymatic reaction. Lipase has better enantioselectivity with increasing rotating speed because of the corresponding increase in *E*. To eliminate the effect of external diffusion on the reaction, a speed of 12.6 ×g is sufficient, and was considered as the optimal rotating speed. The optimal rotation speed of the free enzyme and Fe<sub>3</sub>O<sub>4</sub>-CTS-glutaraldehyde-lipase was 12.6 ×g, because they can uniformly disperse in the reaction system at this rotating speed.

### 4. Effect of Magnetic Field Intensity on the Activity of Fe<sub>3</sub>O<sub>4</sub>-CTS-glutaraldehyde-lipase

Fig. 5 shows that the conversion increased initially and then decreased with the increasing magnetic field intensity in the case of Fe<sub>3</sub>O<sub>4</sub>-CTS-glutaraldehyde-lipase. When the magnetic field intensity was less than 12 Gs, Fe<sub>3</sub>O<sub>4</sub>-CTS-glutaraldehyde-lipase was in an activated state and the conversion increased on increasing the magnetic field intensity. However, when the magnetic field intensity exceeded 12 Gs, the conversion rate started to decrease. Fe<sub>3</sub>O<sub>4</sub>-CTS-glutaraldehyde-lipase generated an induced magnetic field under the action of the external magnetic field. The interaction between these magnetic fields affected the spatial conformation of the enzyme and brought about changes in the enzyme activity.

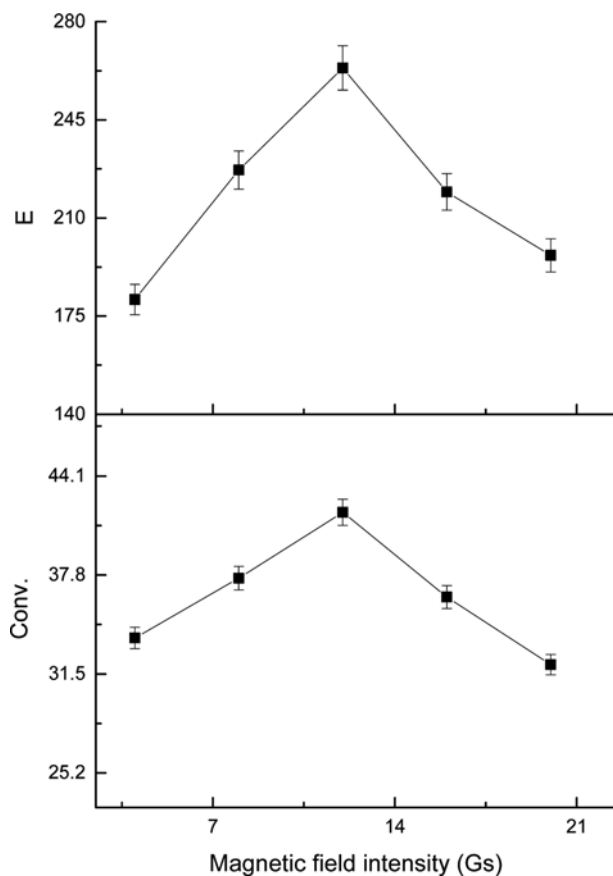


Fig. 5. Effect of the alternating magnetic field strength on the activity of the Fe<sub>3</sub>O<sub>4</sub>-CTS-glutaraldehyde-lipase (Magnetic field frequency: 500 Hz).

The optimal magnetic field frequency and magnetic field intensity was determined to be 500 Hz and 12 Gs, respectively. The conversion, enantiomeric excess of (*R*)-*N*-(1-phenylethyl)acetamide, and *E* value reached 41.8%, 98.4%, and 264, respectively. The conversion and *E* of (*R*)-*N*-(1-phenylethyl)acetamide under the magnetic field were higher than without magnetic field; the enantiomeric excess was 98.4%.

### 5. Reuse of Fe<sub>3</sub>O<sub>4</sub>-CTS-glutaraldehyde-lipase and Free Lipase

Reusability is an important indicator for the application of immobilized enzymes. Generally, the number of times immobilized enzyme can be reused is more than that of free lipase. Fe<sub>3</sub>O<sub>4</sub>-CTS-glutaraldehyde-lipase was reused seven times under the optimal reaction conditions and 12 Gs. Fig. 6 shows that the activity of the Fe<sub>3</sub>O<sub>4</sub>-CTS-glutaraldehyde-lipase decreased slowly with increase of reuse time. A small amount of immobilized lipase was lost during the process of the separation and recovery of Fe<sub>3</sub>O<sub>4</sub>-CTS-glutaraldehyde-lipase. In addition, after each recovery, a small number of immobilized lipase molecules were falling off or lost during the washing process. The apparent relative vitality decreased during the repeated washing. The activity of Fe<sub>3</sub>O<sub>4</sub>-CTS-glutaraldehyde-lipase was maintained at 60% after reusing seven times. Meanwhile, free lipase was inactivated after using four times. These results showed that Fe<sub>3</sub>O<sub>4</sub>-CTS-glutaraldehyde-lipase has high operational stability.

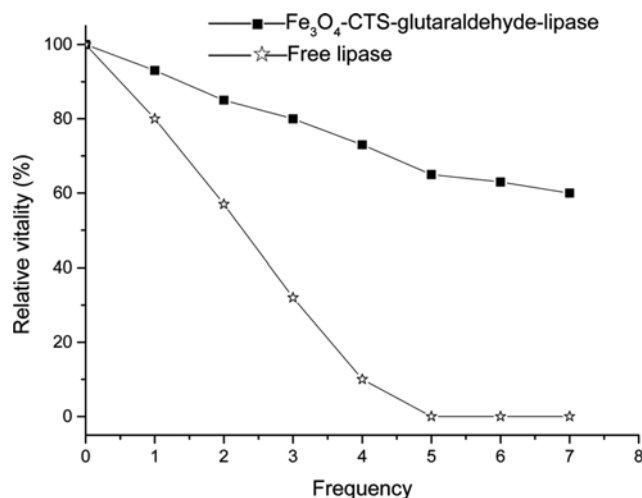


Fig. 6. Reuse of Fe<sub>3</sub>O<sub>4</sub>-CTS-glutaraldehyde-lipase and free lipase.



Scheme 1. Simplified substrate reaction scheme (B, vinyl acetate; E, enzyme; P, Acetaldehyde; A<sub>R</sub>, *R*-phenylethylamine; Q<sub>R</sub>, (*R*)-*N*-(1-phenylethyl)acetamide; EB, enzyme-ester complex; EBA<sub>R</sub>, complex of enzyme-ester and A<sub>R</sub>; EBQ<sub>R</sub>, complex of enzyme-ester and Q<sub>R</sub>).

### 6. Development of Kinetic Model of Selective Acetylation Using Fe<sub>3</sub>O<sub>4</sub>-CTS-glutaraldehyde-lipase

A kinetic model based on the ping-pong bi-bi mechanism [47] was developed by considering the competition of both substrate enantiomers for the active site to describe the kinetic behavior of the lipase-catalyzed enantiomer-selective acylation in this study. The rate equation for initial conditions, is as follows:

$$v = \frac{v_{max}[A]_R[B]}{K_B + K_A[B] + K_B[A]_R + [A]_R[B]} \quad (2)$$

where, *v* is the rate of reaction, *v*<sub>max</sub> maximum rate of reaction, [A]<sub>R</sub>, initial concentration of (*R*)-phenylethylamine, [B], initial concentration of vinyl acetate, *K*<sub>A</sub>, Michaelis constant for (*R*)-phenylethylamine, and *K*<sub>B</sub> is the Michaelis constant for vinyl acetate.

The King-Altman plot of this model is illustrated in Scheme 1. In this model, vinyl acetate (B) bonded to the enzyme (E) and formed a non-covalent enzyme ester intermediate complex (EB). The substrate, (*R*)-phenylethylamine (A<sub>R</sub>), bonded to the enzyme ester intermediate (EB) and formed another complex (EBA<sub>R</sub>), which again underwent isomerization to the ester-enzyme complexes, and finally dissociated into the product, (*R*)-*N*-(1-phenylethyl)acetamide (Q<sub>R</sub>), acetaldehyde (P) and the enzyme.

Using MATLAB to simulate the processes and the six parameters are obtained.

The kinetic parameters obtained for the immobilized lipase by fitting experimental data were as follows: *V*<sub>max</sub>=1.62×10<sup>-2</sup> mM/min, *K*<sub>A</sub>=2.84×10<sup>-4</sup> mM, *K*<sub>B</sub>=0.58 mM.

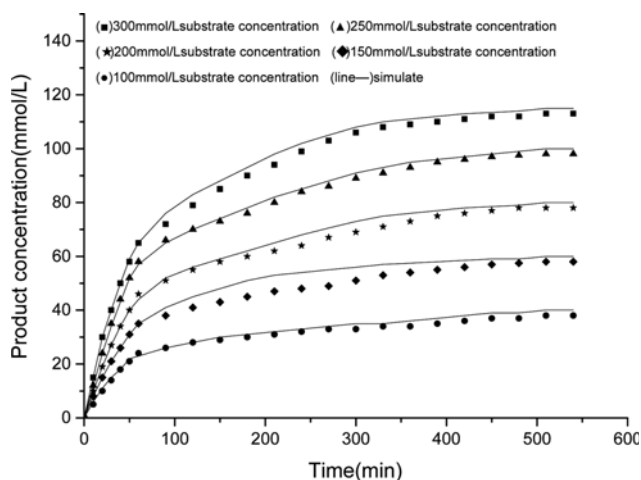


Fig. 7. Comparison of  $\text{Fe}_3\text{O}_4$ -CTS-glutaraldehyde-lipase simulated values with the experimental data of product concentration.

The kinetic model is expressed as follows:

$$v = \frac{0.162 \times [A]_R \times [B]}{0.58 + 2.84 \times 10^{-4} [B] + 0.58 \times [A]_R + [A]_R [B]} \quad (3)$$

The comparison of Fig. 7 confirms that the model data fit well with the experimental data when the substrate concentration was 100–300 mmol/L. Therefore, this model would be useful in the range of experimental substrate concentrations for this kind of acylation reaction catalyzed by immobilized lipase in solvent-free system.

## CONCLUSION

In a solvent-free system, 1-phenylethylamine was resolved by lipase using vinyl acetate as the acyl donor.  $\text{Fe}_3\text{O}_4$ -CTS-glutaraldehyde-lipase, as magnetic chitosan microspheres, was prepared and used for the resolution of racemic 1-phenylethylamine by enantiomer-selective acetylation under an alternating magnetic field. The influence of various factors on the preparation of  $\text{Fe}_3\text{O}_4$ -CTS-glutaraldehyde-lipase was investigated. The optimum immobilization conditions for the preparation of  $\text{Fe}_3\text{O}_4$ -CTS-glutaraldehyde-lipase were 2.4 mg/mL lipase, 10 mg/mL  $\text{Fe}_3\text{O}_4$ -CTS-glutaraldehyde, pH 8.5, 35 °C, 3 h. The loading amount of lipase and the specific activity were 132 mg/g carrier and 48 U/g. The magnetic, physicochemical, and textural characteristics of  $\text{Fe}_3\text{O}_4$ -CTS-glutaraldehyde-lipase were assessed by FT-IR, XRD, and SEM.

The influence of enantiomer-selective acetylation reaction conditions on the conversion by free lipase and  $\text{Fe}_3\text{O}_4$ -CTS-glutaraldehyde-lipase was studied in a shaker incubator. The result showed that immobilization of the enzyme improved the thermal stability of the enzyme. The *ee*(*R*)-**2a** value reached 98.4% using  $\text{Fe}_3\text{O}_4$ -CTS-glutaraldehyde-lipase, which was the same as using free lipase. Furthermore, the stereoselectivity of  $\text{Fe}_3\text{O}_4$ -CTS-glutaraldehyde-lipase was the same as that of free lipase.

The activity of  $\text{Fe}_3\text{O}_4$ -CTS-glutaraldehyde-lipase exposed to an external alternating magnetic field was also measured. It was found that the activity of  $\text{Fe}_3\text{O}_4$ -CTS-glutaraldehyde-lipase increased with the increasing magnetic field intensity until 500 Hz, 12 Gs. How-

ever, out of this range a sharp decrease in the activity was detected. Using  $\text{Fe}_3\text{O}_4$ -CTS-glutaraldehyde-lipase, the conversion under 500 Hz magnetic field frequency and 12 Gs magnetic field intensity alternating magnetic reached 41.8%, while the conversion in the shaker incubator was 37.8%. This indicated that the conversion and activity of  $\text{Fe}_3\text{O}_4$ -CTS-glutaraldehyde-lipase were improved under an alternating magnetic field. Reuse of  $\text{Fe}_3\text{O}_4$ -CTS-glutaraldehyde-lipase under 500 Hz magnetic field frequency and 12 Gs magnetic field intensity alternating magnetic was studied and compared to the reuse of free lipase agitated in a shaker incubator. The result showed that  $\text{Fe}_3\text{O}_4$ -CTS-glutaraldehyde-lipase could be reused seven times, and its activity was still maintained at 60%. On the other hand, the activity of free lipase was maintained at 10% after being reused four times. Thus,  $\text{Fe}_3\text{O}_4$ -CTS-glutaraldehyde-lipase could be reused well and contribute to improved productive efficiency. Pääviö et al. [48] reported the preparative kinetic resolution of rac-**1a** (2 mmol) with isopropyl methoxyacetate (2 mmol) and Novozyme 435 (25 mg) under solvent-free condition in the presence of molecular sieves (50 mg) at 23 °C. The isolated yield and *ee*(*R*)-**2a** reached 48% and 97%. The reuse stability of Novozyme 435 was shown to be poor. The *ee*(*R*)-**2a** gained in our research was 98.4% higher than 97% reported by Pääviö et al. The activity of  $\text{Fe}_3\text{O}_4$ -CTS-glutaraldehyde-lipase was maintained at 60% after reusing seven times. These results showed that  $\text{Fe}_3\text{O}_4$ -CTS-glutaraldehyde-lipase has high operational stability.  $\text{Fe}_3\text{O}_4$ -CTS-glutaraldehyde-lipase has magnetic properties during the separation process, which is suitable for separation after reaction.

A kinetic model for the  $\text{Fe}_3\text{O}_4$ -CTS-glutaraldehyde-lipase catalyzed resolution of 1-phenylethylamine was developed based on the ping-pong bi-bi mechanism. The simulated data of the model fitted the experimental data well. Such a kinetic model can be used as the basis for process engineering studies and for the development of biocatalysts for industrial applications.

## ACKNOWLEDGEMENT

We thank the Natural Science Foundation of Zhejiang Province (LY15B060005) and Huahai Innovation Plan (SR0P) of Zhejiang University of Technology for the financial support.

## REFERENCES

1. M. Cammenberg, K. Hult and S. Park, *ChemBiochem*, **7**(11), 1745 (2006).
2. A. A. Boezio, J. Pytkowicz, A. Côté and A. B. Charette, *J. Am. Chem. Soc.*, **35**(12), 14260 (2004).
3. R. L. Hanson, B. L. Davis, Y. J. Chen, S. L. Goldberg, W. L. Parker, T. P. Tully, M. A. Montana and R. N. Patal, *Adv. Synth. Catal.*, **350**(9), 1367 (2008).
4. D. R. Artis, I. S. Cho and J. M. Muchowski, *Can. J. Chem.*, **70**(6), 1838 (2010).
5. M. Latroche, S. Surblé, C. Serre, C. Mellot-Draznieks, P. L. Llewellyn, J. H. Lee, J. S. Chang, S. H. Jung and G. Férey, *Angew. Chem. Int. Edit.*, **45**(48), 8227 (2010).
6. B. Altava, M. I. Burguete, N. Carbó, J. Escorihuela and S. V. Luis, *Tetrahedron. Asymmetr.*, **21**(8), 982 (2010).

7. K. E. Jaeger and T. Eggert, *Curr. Opin. Biotechnol.*, **13**(4), 390 (2002).
8. F. Hasan, A. A. Shah and A. Hameed, *Enzyme Microb. Technol.*, **39**(2), 235 (2006).
9. K. E. Jaeger and M. T. Reetz, *Trends Biotechnol.*, **16**(9), 396 (1998).
10. A. R. M. Yahya, W. A. Anderson and M. Moo-Young, *Enzyme Microb. Technol.*, **23**(8), 438 (1998).
11. S. Allenmark and A. Ohlsson, *Chirality*, **4**(2), 98 (1992).
12. J. C. Wu, R. L. Hou, Y. Leng, Y. Chow, R. J. Li, M. M. R. Talukder and W. J. Choi, *Biotechnol. Bioproc. E.*, **11**(3), 211 (2006).
13. K. Ditrich, *Cheminform.*, **39**(46), 2283 (2008).
14. A. Adnani, M. Basri and N. Chaibakhsh, *Carbohydr. Res.*, **346**(4), 472 (2011).
15. A. Mustafa, A. Karmali and W. Abdelmoez, *J. Clean. Prod.*, **137**, 953 (2016).
16. K. S. Jaiswal and V. K. Rathod, *Ultrason. Sonochem.*, **40**(PtA), 727 (2018).
17. F. Uthoff, A. Reimer, A. Liese and H. Gröger, *Sustain Chem. Pharm.*, **5**, 42 (2017).
18. S. L. Gilani, G. D. Najafpour, A. Moghadamnia and A. H. Kamaruddin, *J. Mol. Catal. B: Enzym.*, **133**, 144 (2016).
19. W. Xie and J. Wang, *Biomass Bioenerg.*, **36**(328), 373 (2012).
20. B. B. Romdhane, Z. B. Romdhane, A. Gargouri and H. Belghith, *J. Mol. Catal. B: Enzym.*, **68**(3-4), 230 (2011).
21. J. N. Talbert, L. S. Wang, B. Duncan, Y. Jeong, S. M. Andler, V. M. Rotello and J. M. Goddard, *Biomacromolecules*, **15**(11), 3915 (2014).
22. Z. Y. Qu, F. L. Hu, K. M. Chen, Z. Q. Duan, H. C. Gu and H. Xu, *J. Colloid Interface Sci.*, **398**(19), 82 (2013).
23. E. T. Hwang and M. B. Gu, *Eng. Life Sci.*, **13**(1), 49 (2013).
24. P. Ye, Z. K. Xu, A. F. Che, J. Wu and P. Seta, *Biomaterials*, **26**(32), 6394 (2005).
25. B. B. Romdhane, Z. B. Romdhane, A. Gargouri and H. Belghith, *J. Mol. Catal. B: Enzym.*, **68**(3-4), 230 (2011).
26. M. F. G. Manzano and C. I. A. Igarzabal, *J. Mol. Catal. B: Enzym.*, **72**(1-2), 28 (2011).
27. X. Y. Wang, X. P. Jiang, Y. Li, S. Zeng and Y. W. Zhang, *Int. J. Biol. Macromol.*, **75**, 44 (2015).
28. H. Noureddini, X. Gao and R. S. Philkana, *Bioresour. Technol.*, **96**(7), 769 (2004).
29. C. H. Kuo, Y. C. Liu, C. M. J. Chang, J. H. Chen, C. Chang and C. J. Shieh, *Carbohydr Polym.*, **87**(4), 2538 (2012).
30. G. Dodi, D. Hritcu, G. Lisa and M. I. Popa, *Chem. Eng. J.*, **203**(5), 130 (2012).
31. G. Bayramoglu, M. Yilmaz and A. M. Yakup, *Bioprocess Biosyst. Eng.*, **33**(4), 439 (2010).
32. O. L. Tavano, R. Fernandez-Lafuente, A. J. Goulart and R. Monti, *Process. Biochem.*, **48**(7), 1054 (2013).
33. D. I. Bezbradica, C. Mateo and J. M. Guisan, *J. Mol. Catal. B: Enzym.*, **102**(14), 218 (2014).
34. J. Zhi, Y. Wang, Y. Lu, J. Ma and G. Luo, *React. Funct. Polym.*, **66**(12), 1552 (2006).
35. E. B. Denkbaş, E. Kiliçay, C. Birlikseven and E. Öztürk, *React. Funct. Polym.*, **50**(3), 225 (2002).
36. W. Xie and J. Wang, *Biomass Bioenerg.*, **36**(328), 373 (2012).
37. W. J. Ting, K. Y. Tung, R. Giridhar and T. Wu, *J. Mo. Catal. B: Enzym.*, **42**(1), 32 (2006).
38. F. Gros, S. Baup and M. Aurousseau, *Powder Technol.*, **183**(2), 152 (2008).
39. M. Q. Zheng, Z. G. Su, X. Y. Ji, G. H. Ma, P. Wang and S. P. Zhang, *J. Biotechnol.*, **168**(2), 212 (2013).
40. X. J. Janssen, A. J. Schellekens, K. van Ommering, L. J. van Ijzen-doorna and M. W. Prins, *Biosens. Bioelectron.*, **24**(7), 1937 (2009).
41. P. M. Guo, F. H. Huang, Q. D. Huang and C. Zheng, *J. Am. Oil Chem. Soc.*, **55**(1), 561 (2013).
42. C. S. Chen, Y. Fujimoto, G. Girdaukas and C. J. Sih, *J. Am. Chem. Soc.*, **104**(25), 7294 (1982).
43. M. M. Bradford, *Anal. Biochem.*, **72**(s 1-2), 248 (1976).
44. A. Baghban, M. Heidarzadeh, E. Doustkhah, S. Rostamnia and P. F. Rezaei, *Int. J. Biol. Macromol.*, **103**, 1194 (2017).
45. C. L. Pan, B. Hu, W. Li, Y. Sun, H. Ye and X. X. Zeng, *J. Mol. Catal. B: Enzym.*, **61**(3-4), 208 (2009).
46. Q. K. Zhang, J. Q. Kang, B. Yang, L. Z. Zhao, Z. S. Hou and B. Tang, *Chinese. J. Catal.*, **37**(3), 389 (2016).
47. G. D. Yadav and A. H. Trivedi, *Enzyme Microb. Technol.*, **32**(7), 783 (2003).
48. M. Pääviö, P. Perkiö and L. T. Kanerva, *Tetrahedron. Asymmetr.*, **23**(3-4), 230 (2012).